



On-axis average intensity of hypergeometric-Gaussian type propagating in a turbulent atmosphere

F. Khannous¹, M. Boustimi², H. Nebdi¹, A. Belafhal^{1*}

¹Laboratory of Nuclear, Atomic and Molecular Physics
Department of Physics, Faculty of Sciences, Chouaib Doukkali University,
P. B 20, 24000 El Jadida, Morocco

²Physics Department, College of Applied Sciences, Umm Al-Qura University,
P.O. Box : 715, Makkah 21955, Saudi Arabia.

Received 1 Sept 2015, Revised 28 Sept 2015, Accepted 28 Sept 2015

* Corresponding authors: belafhal@gmail.com

Abstract

In this study, the spreading of the hypergeometric-Gaussian type II beams in a turbulent atmosphere is developed in the paraxial approximation. Using the extended Huygens-Fresnel integral formula and based on the expression of the hard aperture, the theoretically of average intensity of the hypergeometric-Gaussian type II beams is derived. The axial average intensity profile is evaluated by altering the beam orders, the beams waist width, the turbulence strength, the radius of an aperture, the wavelength and the propagation distance. Numerical results show that these parameters have an interesting effect on intensity profile. Also, some special cases of average intensity of the hypergeometric-Gaussian type II beams are been extracted from the obtained results.

Keywords: Hypergeometric-Gaussian type II beams; Huygens-Fresnel integral; Turbulent atmosphere.

PACS: 42.68.Bz, 42.60.Jf

1. Introduction

More recently, such a new family of laser beams called the hypergeometric-Gaussian type II (HyGG-II) beams was introduced by Karimi et al. [1]. These beams are considered as a solution of paraxial wave equation like others kinds laser beams, as Bessel-Gauss (BG), Hypergeometric, Hypergeometric-Gaussian (HyGG), elegant Laguerre-Gauss (eLG), superposition of tow modified Bessel (MQBG), Hermite-Laguerre-Gaussian, and Mathieu beams. Under strong focusing, the HyGG-II beams carrying finite power and having better features than the BG beams. The HyGG, eLG, and MQBG beams can be regarded as special cases of the HyGG-II beams under some appropriate conditions of the source parameters. This beams family has a profile of intensity similar to dark hollow beams at the input plane.

During past years, the spreading of laser beams in a turbulent atmosphere has been widely studied both experimentally and theoretically due to their many practical applications [2-5]. When a laser beam propagates through the atmosphere, its quality is affected by turbulence. Consequently, it is important to determinate the propagation properties, such as average intensity, spreading, scintillation, propagation factor, spectral changes, and beam wander of a laser beam then its propagation in turbulent medium. Recently, a variety of investigations has been focused to develop and analyze the effect of a turbulent atmosphere on the propagation of various kinds laser beams [6-14], such as Li's flat-topped [6], Bessel-modulated Gaussian [7], anomalous hollow [8], Ince-Gaussian beams [9], Hermite-Laguerre-Gaussian [10], and elegant Laguerre-Gaussian beams [11]. Up to now, to our knowledge, the average intensity of HyGG-II beams in a turbulent atmosphere has not been studied.

In this paper, we study the variations of axial intensity distribution of HyGG-II beams in a turbulent atmospheric and analyze the effect of the input and output parameters. An analytical expression of the axial intensity is derived by using the extended Huygens-Fresnel integral formula. Numerical results are given by using the obtained equation. Finally, we outlined this paper by some conclusions.

2. Propagation properties of HyGG-II beams in a turbulent atmosphere

In this section, we will treat the propagation of HyGG-II beams in a turbulent atmosphere by determination of the analytical expression of the average intensity. Using the paraxial form of the extended Huygens-Fresnel, the average intensity at the output plane is given by [7-10]

$$\langle I(\vec{\rho}, z) \rangle = \frac{k^2}{4\pi^2 z^2} \iint_0^a \iint_0^{2\pi} \iint_0^{2\pi} E(\vec{r}_1, 0) E^*(\vec{r}_2, 0) \exp \left[\frac{ik}{2z} \left((\vec{r}_1 - \vec{\rho})^2 - (\vec{r}_2 - \vec{\rho})^2 \right) \right] \langle \exp \left[\psi(\vec{r}_1, \vec{\rho}) + \psi^*(\vec{r}_2, \vec{\rho}) \right] \rangle d\vec{r}_1 d\vec{r}_2, \quad (1)$$

where * is the complex conjugate, $\langle \rangle$ is the ensemble average over the turbulent media, a is the radius of the aperture, $\psi(\vec{r}, \vec{\rho})$ denotes, in the Rytov model, the random complex phase of spherical wave propagating from the source plane to the output plane, $E(\vec{r}, 0)$ is the electric field of the laser beam at the source plane, z is the distance between the source plane and the receiver plane, $\vec{r}_1 = (r_1, \theta)$, and $\vec{\rho} = (\rho, \psi)$. The ensemble average term in last equation can be expressed as [2]

$$\langle \exp \left[\psi(\vec{r}_1, \vec{\rho}) + \psi^*(\vec{r}_2, \vec{\rho}) \right] \rangle = \exp \left[-\frac{1}{\rho_0^2} (\vec{r}_1 - \vec{r}_2)^2 \right], \quad (2)$$

where for the Kolmogorov model, $\rho_0 = (0.545 C_n^2 k^2 z)^{-3/5}$ is the coherence length of a spherical wave propagating in the turbulent medium and C_n^2 is the refractive index structure constant, which characterizes the local strength of the turbulent atmosphere.

The electric field of HyGG-II beams in the cylindrical coordinates system (r, θ, z) at the source plane $z=0$ is expressed by [1]

$$E_m(r, \theta, 0) = \frac{A_0}{\omega_0^{|m|}} e^{i|m|\theta} \exp \left(-\frac{r^2}{\omega_0^2} \sum_{n=0}^{\infty} \frac{\left(\frac{-p}{2} \right)_n}{(|m|+1)_n} \frac{1}{n!} \left(\frac{1}{\omega_0} \right)^{2n} r^{2n+|m|} \right), \quad (3)$$

where A_0 is a complex factor, (r, θ) are the polar coordinates, ω_0 is the waist width of the beam, $\exp(i|m|\theta)$ is the phase term for the beams, p is a real number which represents the parameter that determines the hollowness and m is the topological charge. When $m=p=0$, Eq. (3) is reduced to Gaussian beams, evidently. Figure 1 shows the variation of the intensity at the source plane with different values of hollowness parameter p . It can be seen from this figure that, the decreasing of p leads to more hollowness of the plot. Also, Figure 1 clearly shows that, the profile of the intensity of HyGG-II beams is similar to dark hollow beams.

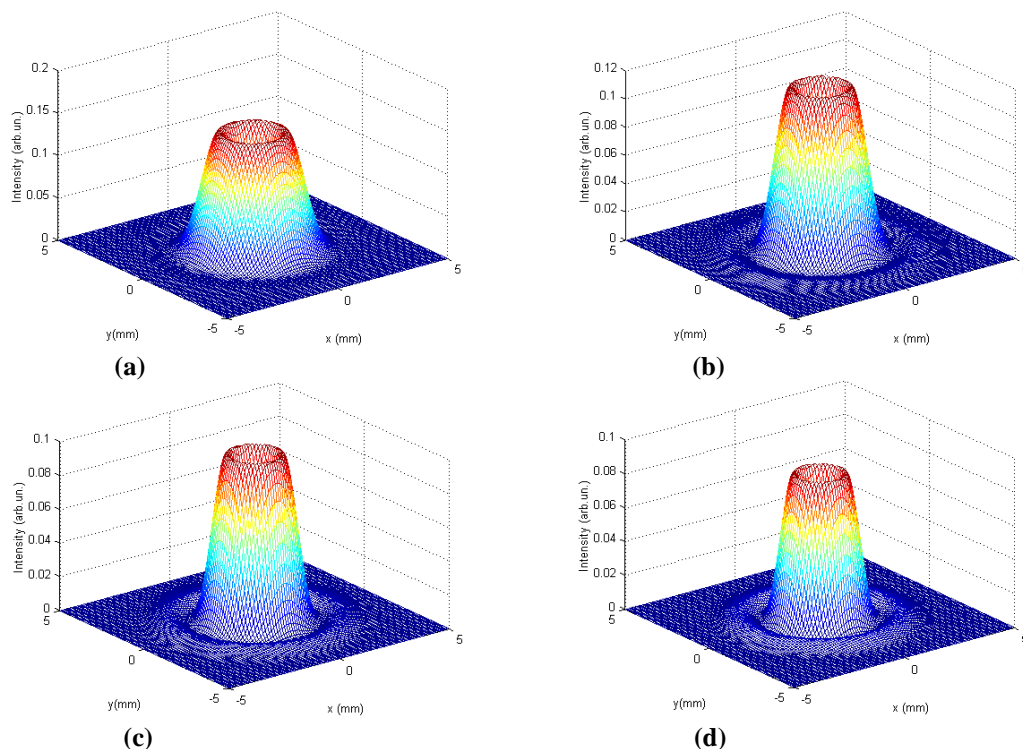


Figure 1: Source plane intensity distribution of HyGG-II beams, with $\omega_0=0.002\text{m}$, $m=1$ and (a) $p=1.2$, (b) $p=2.2$, (c) $p=3.2$, (d) $p=4.2$.

Substituting Eqs. (2) and (3) into Eq. (1), one obtains the average of the intensity at the output plane over the turbulent media

$$\begin{aligned} \langle I(\rho, z) \rangle = & \frac{k^2}{4\pi^2 z^2 \omega_0^{2|m|}} A_0^2 \sum_{n=0}^{\infty} \left(\frac{-P}{2}\right)_n \frac{1}{(m+1)_n} \frac{1}{n!} \left(\frac{1}{\omega_0}\right)^{2n} \sum_{n=0}^{\infty} \left(\frac{-P}{2}\right)_{n'} \frac{1}{(m+1)_{n'}} \frac{1}{n'!} \left(\frac{1}{\omega_0}\right)^{2n'} \\ & \times \int_0^a \int_0^{2\pi} \int_0^{2\pi} e^{i|m|(\theta_1 - \theta_2)} \exp\left[-\left(\frac{1}{\omega_0^2} + \frac{1}{\rho_0^2} - \frac{ik}{2z}\right)r_1^2\right] \exp\left[-\left(\frac{1}{\omega_0^2} + \frac{1}{\rho_0^2} + \frac{ik}{2z}\right)r_2^2\right] \exp\left[\frac{ik}{z}\rho(r_1 \cos(\theta_1 - \psi) - r_2 \cos(\theta_2 - \psi))\right] \\ & \times \exp\left[\frac{2r_1 r_2}{\rho_0^2} \cos(\theta_1 - \theta_2)\right] r_1^{2n+|m|+1} dr_1 d\theta_1 r_2^{2n'+|m|+1} dr_2 d\theta_2. \end{aligned} \quad (4)$$

An exact analytical solution of this equation is not possible because the integral evaluation is complicated. For this reason, in the next section, we will use this last equation to determine only the axial intensity of the considered beams family.

3. Axial intensity of HyGG-II beams in a turbulent atmosphere

We will evaluate the axial intensity distribution of the HyGG-II beams propagating in a turbulent atmosphere. Using of the following expression of the hard aperture function into a finite sum complex Gaussian functions [15]

$$H(r) = \sum_{h=1}^M A_h \exp\left(-\frac{B_h}{a^2} r^2\right), \quad (5)$$

where A_h and B_h denote the expansion and Gaussian coefficients, respectively. M represents the number of the expansion terms and generally is equal to ten.

For the propagation on the axis, we have $\rho=0$, then, substituting Eq. (5) into Eq. (4), we can express the axial intensity in the following form

$$\begin{aligned} \langle I(0, z) \rangle = & \frac{k^2}{4\pi^2 z^2 \omega_0^{2|m|}} A_0^2 \sum_{n=0}^{\infty} \left(\frac{-P}{2}\right)_n \frac{1}{(m+1)_n} \frac{1}{n!} \left(\frac{1}{\omega_0}\right)^{2n} \sum_{n=0}^{\infty} \left(\frac{-P}{2}\right)_{n'} \frac{1}{(m+1)_{n'}} \frac{1}{n'!} \left(\frac{1}{\omega_0}\right)^{2n'} \sum_{h=1}^M A_h \sum_{h=1}^M A_h \\ & \times \int_0^a \int_0^{2\pi} \int_0^{2\pi} e^{i|m|(\theta_1 - \theta_2)} \exp\left[-\left(\frac{1}{\omega_0^2} + \frac{1}{\rho_0^2} + \frac{B_h}{a^2} - \frac{ik}{2z}\right)r_1^2\right] \exp\left[-\left(\frac{1}{\omega_0^2} + \frac{1}{\rho_0^2} + \frac{B_h}{a^2} + \frac{ik}{2z}\right)r_2^2\right] \\ & \times \exp\left[\frac{2r_1 r_2}{\rho_0^2} \cos(\theta_1 - \theta_2)\right] r_1^{2n+|m|+1} dr_1 d\theta_1 r_2^{2n'+|m|+1} dr_2 d\theta_2. \end{aligned} \quad (6)$$

To solve the finite integral in the above equation, we use the following equality [7]

$$\int_0^{2\pi} \exp[-im\theta_1 + x \cos(\theta_1 - \theta_2)] d\theta_1 = 2\pi \exp(-im\theta_2) I_m(x), \quad (7)$$

where I_m is the m - order modified Bessel function. So, Eq. (6) will transform into

$$\begin{aligned} \langle I(0, z) \rangle = & \frac{k^2}{z^2 \omega_0^{2|m|}} A_0^2 \sum_{n=0}^{\infty} \left(\frac{-P}{2}\right)_n \frac{1}{(m+1)_n} \frac{1}{n!} \left(\frac{1}{\omega_0}\right)^{2n} \sum_{n=0}^{\infty} \left(\frac{-P}{2}\right)_{n'} \frac{1}{(m+1)_{n'}} \frac{1}{n'!} \left(\frac{1}{\omega_0}\right)^{2n'} \sum_{h=1}^M A_h \sum_{h=1}^M A_h \\ & \times \int_0^a \int_0^{2\pi} r_1^{2n+|m|+1} r_2^{2n'+|m|+1} \exp(-\beta_1 r_1^2) \exp(-\beta_2 r_2^2) I_{|m|}\left(\frac{2r_1 r_2}{\rho_0^2}\right) dr_1 dr_2, \end{aligned} \quad (8)$$

where

$$\beta_1 = \frac{1}{\omega_0^2} + \frac{1}{\rho_0^2} + \frac{B_h}{a^2} - \frac{ik}{2z}, \quad (9.a)$$

and

$$\beta_2 = \frac{1}{\omega_0^2} + \frac{1}{\rho_0^2} + \frac{B_h}{a^2} + \frac{ik}{2z}. \quad (9.b)$$

Making use of the integral formula [16]

$$\int_0^{\infty} x^{\mu-\frac{1}{2}} e^{-\alpha x} I_{2\nu}(2\beta\sqrt{x}) dx = \frac{\Gamma\left(\nu+\mu+\frac{1}{2}\right)}{\Gamma(2\nu+1)} \beta^{-1} e^{\frac{\beta^2}{2\alpha}} \alpha^{-\mu} M_{-\mu, \nu}\left(\frac{\beta^2}{\alpha}\right), \quad (10)$$

also using the definition of the confluent hypergeometric function [16]

$$M_{x,\delta}(z) = z^{\frac{\delta+1}{2}} e^{-\frac{z}{2}} {}_1F_1\left(\delta - x + \frac{1}{2}; 2\delta + 1; z\right), \quad (11)$$

and after tedious the calculation, Eq. (8) can be simplify by

$$\begin{aligned} \langle I(0, z) \rangle = & \frac{k^2}{z^2 \omega_0^{2|m|}} A_0^2 \frac{\left(\frac{1}{\rho_0^2}\right)^{|m|}}{2\Gamma(|m|+1)} \sum_{n=0}^{\infty} \frac{\left(-\frac{p}{2}\right)_n}{(|m|+1)_n} \frac{1}{n!} \left(\frac{1}{\omega_0}\right)^{2n} \sum_{n=0}^{\infty} \frac{\left(-\frac{p}{2}\right)_n}{(|m|+1)_n} \frac{1}{n!} \left(\frac{1}{\omega_0}\right)^{2n} \sum_{h=1}^M A_h \sum_{h=1}^M A_h \\ & \times \frac{\Gamma(|m|+n+1)}{\beta_2^{|m|+n+1}} \int_0^{\infty} r_1^{2n+2|m|+1} \exp(-\beta_1 r_1^2) {}_1F_1\left(|m|+n+1; |m|+1; \frac{r_1^2}{\rho_0^4 \beta_2}\right) dr_1, \end{aligned} \quad (12)$$

where Γ denotes the gamma function.

Using the identity 7.522 in [16]

$$\int_0^{\infty} x^{\delta-1} \exp(-\mu x) {}_mF_n(\alpha_1, \alpha_2, \dots, \alpha_m; \gamma_1, \gamma_2, \dots, \gamma_n; \lambda x) dx = \Gamma(\delta) \mu^{-\delta} {}_{m+1}F_n\left(\alpha_1, \alpha_2, \dots, \alpha_m; \delta; \gamma_1, \gamma_2, \dots, \gamma_n; \frac{\lambda}{\mu}\right), \quad (13)$$

with $m \leq n, \text{Re } \delta' > 0; \text{Re } \mu' > 0$, if $m < n; \text{Re } \mu' > \lambda$, if $m = n$,

Eq. (12) is equivalent to

$$\begin{aligned} \langle I(0, z) \rangle = & \frac{k^2}{z^2 \omega_0^{2|m|}} A_0^2 \frac{\left(\frac{1}{\rho_0^2}\right)^{|m|}}{2^2 \Gamma(|m|+1)} \sum_{n=0}^{\infty} \frac{\left(-\frac{p}{2}\right)_n}{(|m|+1)_n} \frac{1}{n!} \left(\frac{1}{\omega_0}\right)^{2n} \sum_{n=0}^{\infty} \frac{\left(-\frac{p}{2}\right)_n}{(|m|+1)_n} \frac{1}{n!} \left(\frac{1}{\omega_0}\right)^{2n} \sum_{h=1}^M A_h \sum_{h=1}^M A_h \\ & \times \frac{\Gamma(|m|+n+1) \Gamma(|m|+n+1)}{\beta_2^{|m|+n+1} \beta_1^{|m|+n+1}} {}_2F_1\left(|m|+n+1, |m|+n+1; |m|+1; \frac{1}{\rho_0^4 \beta_1 \beta_2}\right), \end{aligned} \quad (14)$$

where ${}_2F_1(a; b; c; x)$ denotes the hypergeometric function which is defined by ${}_2F_1(a; b; c; x) = \sum_{j=0}^{+\infty} \frac{(a)_j (c)_j}{(b)_j} \frac{x^j}{j!}$.

Eq. (14) represents the analytical expression of the axial intensity of the HyGG-II beams propagating in a turbulent atmosphere. This equation shows that the axial intensity depends on the hollowness parameter, the topological charge, the wavelength, the parameter structure of the turbulence strength and the propagation distance.

There are three special cases of Eq. (14) that one can deduced immediately:

- The first one is the case when $p=m=0$. In this case, Eq. (14) simplifies to

$$\langle I(0, z) \rangle = \frac{k^2}{z^2} A_0^2 \sum_{h=1}^M A_h \sum_{h=1}^M A_h \frac{\rho_0^4}{4 \left[\rho_0^4 \left(\frac{1}{\omega_0^2} + \frac{1}{\rho_0^2} + \frac{B_h}{a^2} - \frac{ik}{2z} \right) \left(\frac{1}{\omega_0^2} + \frac{1}{\rho_0^2} + \frac{B_h}{a^2} + \frac{ik}{2z} \right) - 1 \right]}, \quad (15)$$

which is the axial intensity of a Gaussian beam propagating in a turbulent atmosphere. This result is consistent with Eq. (21) of Ref. [14].

- The second one is the case for $p=-|m|$ a negative number. The HyGG-II beams reduce to a superposition of tow modified Bessel (MQBG) beams. In this case, we can write Eq. (14) in the following form

$$\begin{aligned} \langle I(0, z) \rangle = & \frac{k^2}{z^2 \omega_0^{2|m|}} A_0^2 \frac{\left(\frac{1}{\rho_0^2}\right)^{|m|}}{2^2 \Gamma(|m|+1)} \sum_{n=0}^{\infty} \frac{\left(\frac{|m|}{2}\right)_n}{(|m|+1)_n} \frac{1}{n!} \left(\frac{1}{\omega_0}\right)^{2n} \sum_{n=0}^{\infty} \frac{\left(\frac{|m|}{2}\right)_n}{(|m|+1)_n} \frac{1}{n!} \left(\frac{1}{\omega_0}\right)^{2n} \sum_{h=1}^M A_h \sum_{h=1}^M A_h \\ & \times \frac{\Gamma(|m|+n+1) \Gamma(|m|+n+1)}{\beta_2^{|m|+n+1} \beta_1^{|m|+n+1}} {}_2F_1\left(|m|+n+1, |m|+n+1; |m|+1; \frac{1}{\rho_0^4 \beta_1 \beta_2}\right). \end{aligned} \quad (16)$$

This last equation represents the axial intensity of MQBG beams propagating in a turbulent medium.

- The third one is the case for $p \geq 0$ even integer number. We find the analytical expression of the axial intensity of eLG beams propagating in a turbulent atmosphere.

4. Results and discussions

In this section, we investigate the propagation properties of the HyGG-II beams in turbulence media, using the analytical expression derived in the previous section. In the intensity profile, we have normalized all the intensity results with respect their maxima.

Figure 2 explores the effect of turbulence on distribution of axial intensity by changing the turbulent strengths. It can be seen that, the distribution of the intensity of HyGG-II beams increases up to a corresponding maximum z_{max} then decreases with the increasing of propagation distance.

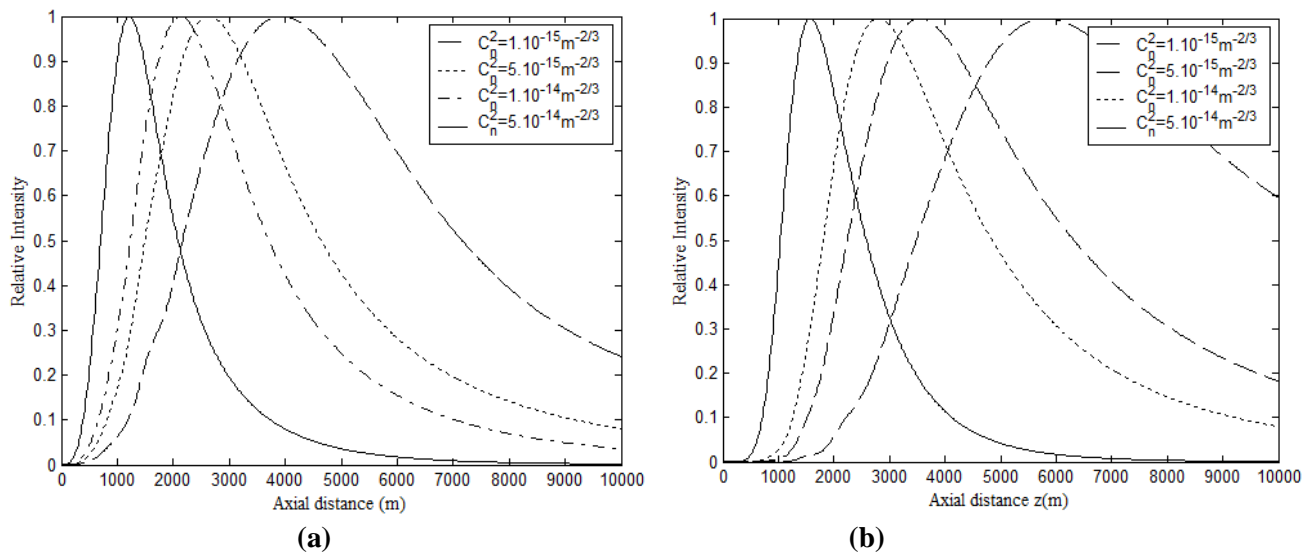


Figure 2: Normalized distribution of the on-axis average intensity of HyGG-II beams for two values of the topological charge (a) $m=1$, (b) $m=2$, with several different turbulent strengths. The others parameters are $\omega_0=0.05m$, $a=0.15m$, $p=2.2$, and $\lambda=1550nm$.

This corresponding maximum z_{max} of the profile increases with decreasing of the turbulent strengths. Also, from this figure, it can be observe that when the topological charge increases the average intensity increases.

We illustrate also in Figure 3 the on-axis average intensity for HyGG-II beams with different values of the hollowness parameter. From this figure, plotted as function of the axial distance from 0 to 10km, it is clear for every value of p , the corresponding maximum z_{max} of the normalized distribution of the intensity decreases while the hollowness parameter increases.

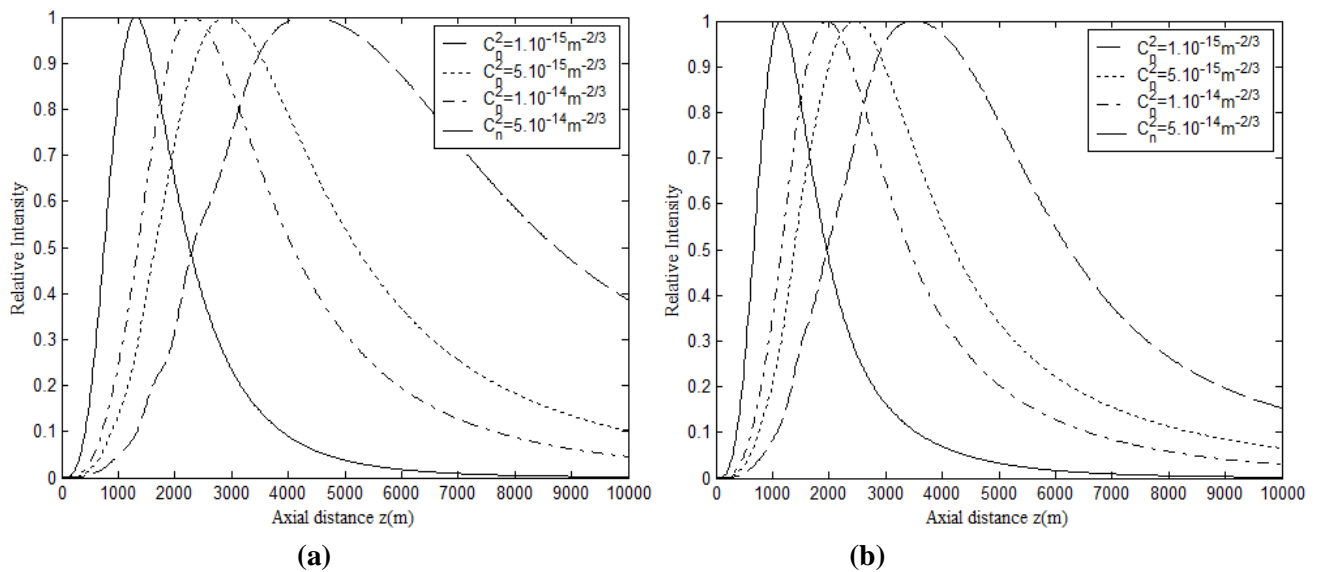


Figure 3: Normalized distribution of the on-axis average intensity of HyGG-II beams for two values of p (a) $p=1.2$, (b) $p=3.2$, with several different turbulent strengths. The others parameters are $\omega_0=0.05m$, $a=0.15m$, $m=1$, and $\lambda=1550nm$.

In Figure 4, normalized average intensity of HyGG-II beams is plotted as a function of the axial distance z at several wavelengths, in a turbulent atmosphere for selected values of the topological charge. Figure 4 shows that, the on-axis average intensity oscillates in the near field ($z < 1000\text{m}$). The increased levels of wavelength, accelerates the oscillations number. Also, from this figure, it is clear that the profile of the on-axis intensity and the position of its maximum depend on the values of the wavelength. Furthermore, it can be seen that, although the variation of average intensity depends on the emitting aperture radius, as it increases with its increase. Finally, we give in Figure 5 the evolution of the normalized intensity of HyGG-II beams through a turbulent atmosphere. Figure 5 demonstrates clearly that, the increase of the beam waist width leads to the increase of the average intensity up to a corresponding maximum z_{max} then decreases with the increasing of propagation distance. From this figure, we can also observe that, the position of corresponding maximum z_{max} increases with the increasing of the beam waist width.

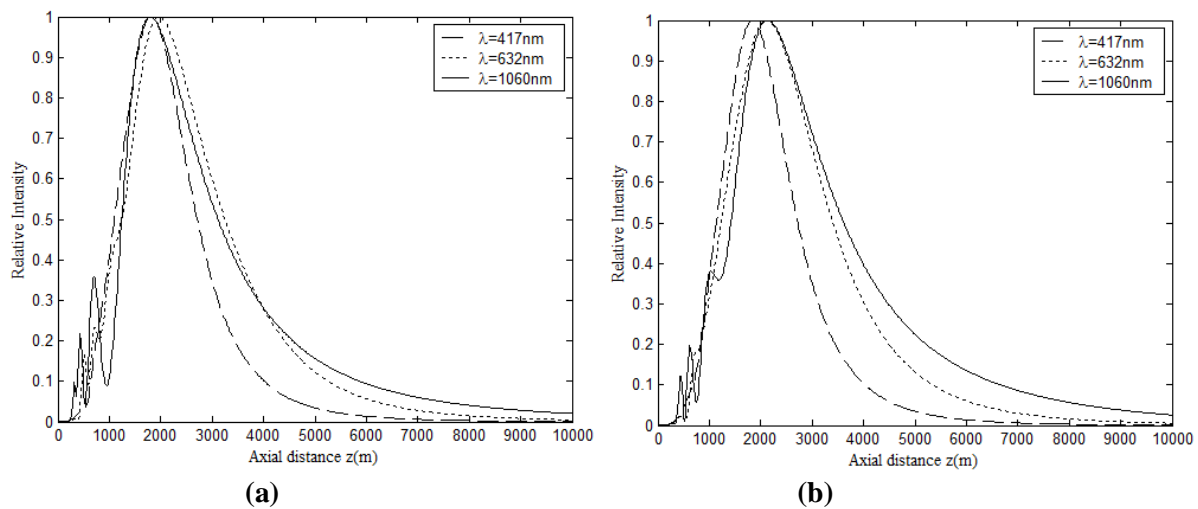


Figure 4: Normalized distribution of the on-axis average intensity of HyGG-II beams for two values of the emitting aperture radius (a) $a=0.05\text{m}$, (b) $a=0.06\text{m}$, with several different values of λ . The others parameters are $\omega_0=0.05\text{m}$, $m=1$, $p=1.2$, and $C_n^2 = 1.10^{-14} \text{m}^{-2/3}$.

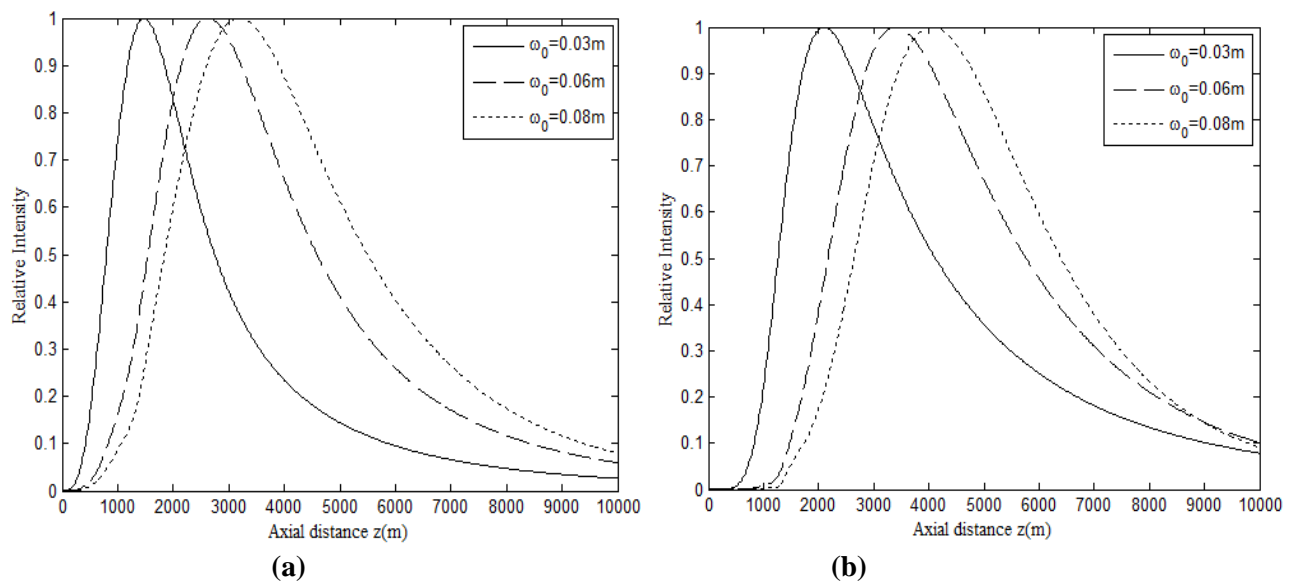


Figure 5: Normalized distribution of the on-axis average intensity of HyGG-II beams for two values of topological charge (a) $m=1$, (b) $m=2$, with several different values of waist width. The others parameters are $\lambda=1550\text{nm}$, $a=0.15\text{m}$, $p=1.2$, and $C_n^2 = 1.10^{-14} \text{m}^{-2/3}$.

Conclusions

Based on the extended Huygens-Fresnel integral formula and the expression of the hard aperture, the axial propagation properties of HyGG-II beams in a turbulent atmospheric are investigated. The analytical expression for the average intensity of HyGG-II beams spreading through a turbulent medium has been obtained. The results show that the axial intensity of HyGG-II beams changes with the variation of the beam order, the topological charge, the wavelengths, the turbulent strengths, and the beam waist width. Also, the average intensity of the fundamental Gaussian, the superposition of two modified Bessel, and the elegant Laguerre-Gauss beams are been extracted from the obtained results as the special cases of the HyGG-II beams.

References

1. Karimi E., Piccirillo B., Marrucci L., Santamato E., *Opt. Express* 16 (2008) 21069-21075.
2. Andrews L., Phillips R., *Laser Beam Propagation Through Random Media*, SPIE Press, Washington, (1998).
3. Eyyuboğlu H.T., Baykal Y., *Appl. Opt.* 44 (2005) 976- 983.
4. Arpali C., Yazicioglu C., Eyyuboglu H.T., Arpali S.A., Baykal Y., *Opt. Express* 14 (2006) 8919-8928.
5. Cai Y., He S., *Opt. Express* 14 (2006) 1353-1367.
6. Kinani K., Ez-zariy L., Chafiq A., Nebdi H., Belafhal A., *Phys. Chem. News* 61 (2011) 24-33.
7. Belafhal A., Hennani S., Ez-zariy L., Chafiq A., Khouilid M., *Phys. Chem. News* 62 (2011) 36-43.
8. Cai Y., Eyyuboglu H.T., Baykal Y., *Opt. Commun.* 281 (2008) 5291–5297.
9. Eyyuboğlu H.T., *Appl. Opt.* 53 (2014) 2290-2296.
10. Ni Y., Wang X., Zhou G., *Appl. Phys. B* 111 (2013) 131–140.
11. Qu J., Zhong Y., Cui Z., Cai Y., *Opt. Commun.* 283 (2010) 2772–2781.
12. Zhou G., *Opt. Express* 19 (2011) 3945-3951.
13. Alavinejad M., Ghafary B., Kashani F.D., *Optics and Lasers in Engineering* 46 (2008) 1-5.
14. Cang J., Zhang Y., *Optik* 121 (2010) 239-245.
15. Wen J. J., Breazeal M. A., *J. Acoust. Soc. Am.* 83 (1998) 1752-1756.
16. Gradshteyn I. S., Ryzhik I. M., *Tables of Integrals, Series and Products*, 5th ed, (Academic. Press, New York, 1994).

(2015) ; <http://www.jmaterenvironsci.com>